Relaxation rate of a stochastic spreading process in a closed ring

Daniel Hurowitz and Doron Cohen
Department of Physics, Ben-Gurion University of the Negev, Beer-Sheva, Israel
(Received 20 March 2016; published 29 June 2016)

The relaxation process of a diffusive ring becomes underdamped if the bias (so-called affinity) exceeds a critical threshold value, also known as the delocalization transition. This is related to the spectral properties of the pertinent stochastic kernel. We find the dependence of the relaxation rate on the affinity and on the length of the ring. Additionally we study the implications of introducing a weak link into the circuit and illuminate some subtleties that arise while taking the continuum limit of the discrete model.

DOI: 10.1103/PhysRevE.93.062143

I. INTRODUCTION

In the absence of topology the relaxation time of a stochastic sample is determined either by the diffusion or by the drift, depending on whether the bias is small or large, respectively. In contrast, in a topologically closed circuit, as the bias is increased, the relaxation becomes underdamped with relaxation rate that is determined by the diffusion and not by the drift. In related applications the "circuit" might be a chemical cycle, and the "bias" is the so-called affinity of the cycle.

In the present work we consider a minimal model for a topologically closed circuit, namely, an N-site ring with nearest-neighbor hopping. The dynamics can be regarded as a stochastic process in which a particle hops from site to site. The rate equation for the site occupation probabilities $\boldsymbol{p} = \{p_n\}$ can be written in matrix notation as

$$\frac{d\boldsymbol{p}}{dt} = \boldsymbol{W}\boldsymbol{p} \tag{1}$$

If the ring were opened, then the $N \to \infty$ limit would correspond to Sinai's spreading problem [1–4], also known as a random walk in a random environment, where the transition rates are allowed to be asymmetric. Such models have diverse applications, notably in biophysical contexts of populations biology [5,6], pulling pinned polymers and DNA unzipping [7,8], and in particular with regard to molecular motors [9–12].

In the absence of topology, $\boldsymbol{W}$ is *similar* to a real symmetric matrix, and the relaxation spectrum is *real* (i.e., damped relaxation). Alas, for a ring the affinity is a topological invariant that cannot be gauged away, analogous to the Aharonov-Bohm flux, and the relaxation spectrum might become *complex* (i.e., underdamped relaxation). Thus the theme that we address here is related to the study of non-Hermitian quantum Hamiltonians [13–15]. In a previous work [16] we illuminated the relation between the sliding transition and the complexity threshold, i.e., the "delocalization transition," as the affinity is increased.

The outline is as follows: In Sec. II we discuss the relaxation in the case of a homogeneously disordered diffusive sample, contrasting nontrivial topology (ring) with simple geometry (box). The effect of disorder is demonstrated in Sec. III, where heuristic considerations are used in order to explain the dependence of the relaxation rate on the affinity and on the length of the ring. In Sec. IV we discuss the delocalization transition. Namely, we find the threshold value of the affinity beyond which the relaxation becomes underdamped. Then we extract the relaxation rate from the characteristic equation using an "electrostatic picture." As explained in Sec. V the same picture can be used to address sparse disorder. This motivates the analysis in Secs. VI and VII of the relaxation in a ring that has an additional weak link that forms a bottleneck for diffusion, though not blocking it completely. Several appendices are provided to make the presentation self-contained.

II. DIFFUSIVE SAMPLE: RING VERSUS BOX

The rate equation, Eq. (1), involves a matrix $\boldsymbol{W}$ whose off-diagonal elements are the transition rates w_{nm}, and whose diagonal elements are $-\gamma_n$ such that each column sums to zero. Via diagonalization one can find the eigenvalues $\{-\lambda_\nu\}$. Irrespective of the model's details there always exists an eigenvalue $\lambda_0 = 0$ that corresponds to the nonequilibrium steady state (NESS). The other eigenvalues reflect the relaxation modes of the system: they have positive $\mathrm{Re}[\lambda_\nu]$ and might be complex. Complexity of the low eigenvalues implies an underdamped relaxation.

For a clean ring and with nearest-neighbor hopping, the rates are uniform but asymmetric and are equal to $\overrightarrow{w} = we^{s/2}$ for forward hopping, and $\overleftarrow{w} = we^{-s/2}$ for backward hopping. The $\boldsymbol{W}$ matrix takes the form

$$\boldsymbol{W} = \begin{bmatrix} -\gamma & \overleftarrow{w} & 0 & \cdots & \overrightarrow{w} \\ \overrightarrow{w} & -\gamma & \overleftarrow{w} & \cdots & \cdots \\ 0 & \overrightarrow{w} & -\gamma & \cdots & \cdots \\ \cdots & \cdots & \cdots & \cdots & \cdots \\ \overleftarrow{w} & \cdots & \cdots & \cdots & \cdots \end{bmatrix} \tag{2}$$

with $\gamma = -2w\cosh(s/2)$. Due to translational invariance, this matrix can be written in terms of the momentum operator:

$$\boldsymbol{W} = we^{s/2+i\boldsymbol{P}} + we^{-s/2-i\boldsymbol{P}} - 2w\cosh\left(\frac{s}{2}\right). \tag{3}$$

From here it is easy to see that the eigenvalues are

$$\lambda_\nu = 2w\left[\cosh\left(\frac{s}{2}\right) - \cos\left(\frac{2\pi}{N}\nu + i\frac{s}{2}\right)\right]. \tag{4}$$

The complexity of the $\nu \neq 0$ eigenvalues implies that the relaxation process is not overdamped. A straightforward analysis of the time-dependent spreading process (see, e.g., [17]) shows that the drift velocity and the diffusion coefficient

are given by the following expressions:

$$v_0 = (\overrightarrow{w} - \overleftarrow{w})a = 2wa\sinh(s/2), \tag{5}$$

$$D_0 = \tfrac{1}{2}(\overrightarrow{w} + \overleftarrow{w})a^2 = wa^2\cosh(s/2), \tag{6}$$

where a is the lattice constant. Note that in Eq. (3) we used the lattice constant as a unit of length ($a = 1$) else the following replacement is required: $\boldsymbol{P} \mapsto a\boldsymbol{P}$.

It is convenient to consider the continuum limit of the rate equation, Eq. (1). In this limit we define $D(x) = wa^2$ and $v(x) = swa$, and the continuity equation for the probability density $\rho(x_n) = (1/a)p_n$ becomes the Fokker-Planck diffusion equation:

$$\frac{d\rho}{dt} = -\frac{d}{dx}\left[-D(x)\frac{d\rho}{dx} + v(x)\rho(x)\right]. \tag{7}$$

One can easily find the spectrum of the relaxation modes ($\mathrm{Re}[\lambda_\nu] > 0$) for either ring or box geometry. The length of the segment is $L = Na$, and the boundary conditions are respectively either of Neumann type or periodic. The result is

$$\lambda_\nu[\text{ring}] = \left(\frac{2\pi}{L}\right)^2 D\nu^2 + i\frac{2\pi v}{L}\nu, \tag{8}$$

$$\lambda_\nu[\text{box}] = \left(\frac{\pi}{L}\right)^2 D\nu^2 + \frac{v^2}{4D}, \tag{9}$$

where $\nu = \pm 1, \pm 2, \ldots$ for the ring, while $\nu = 1,2,3,\ldots$ for the box. Clearly Eq. (8) is consistent with Eq. (4). The relaxation rate Γ is determined by the lowest eigenvalue,

$$\Gamma \equiv \mathrm{Re}[\lambda_1]. \tag{10}$$

For the ring it is determined solely by the diffusion coefficient:

$$\Gamma[\text{ring}] = \left(\frac{2\pi}{L}\right)^2 D, \tag{11}$$

while for the box, if the bias is large, it is predominantly determined by the drift:

$$\Gamma[\text{box}] = \left[\left(\frac{\pi}{L}\right)^2 + \left(\frac{v}{2D}\right)^2\right]D. \tag{12}$$

It is important to realize that in the latter case we have a "gap" in the spectrum, meaning that λ_1 does not diminish in the $L \to \infty$ limit; hence the relaxation time is finite.

III. DISORDERED RING

In the presence of disorder, the forward and backward rates across the nth bond are random numbers $\overrightarrow{w}_n$ and $\overleftarrow{w}_n$. Accordingly the diagonal elements of $\boldsymbol{W}$ are random too, namely, $\gamma_n = \overleftarrow{w}_n + \overrightarrow{w}_{n+1}$. By considering the long time limit of the time-dependent spreading process it is still possible to define the drift velocity v and diffusion coefficient D. The results depend in an essential way on the affinity of the cycle,

$$S_{\circlearrowleft} \equiv Ns, \tag{13}$$

where s is defined via the sample average

$$\frac{1}{N}\sum_{n=1}^{N}\ln\left(\frac{\overleftarrow{w}_n}{\overrightarrow{w}_n}\right) \equiv -s. \tag{14}$$

Additionally it is useful to define threshold values s_μ, whose significance is clarified in the next section, via the following expression:

$$\frac{1}{N}\sum_{n=1}^{N}\left(\frac{\overleftarrow{w}_n}{\overrightarrow{w}_n}\right)^\mu \equiv e^{-(s-s_\mu)\mu}. \tag{15}$$

Here, as in [16,17], we assume that the rates are

$$\overrightarrow{w}_n = we^{+\mathcal{E}_n/2}, \tag{16}$$

$$\overleftarrow{w}_n = we^{-\mathcal{E}_n/2}, \tag{17}$$

where the activation energies $\mathcal{E}_n$ are box distributed within $[s-\sigma, s+\sigma]$. Approximating the sample average by an ensemble average the thresholds of Eq. (15) are

$$s_\mu = \frac{1}{\mu}\ln\left(\frac{\sinh(\sigma\mu)}{\sigma\mu}\right). \tag{18}$$

For small μ one obtains $s_\mu \approx (1/6)\mu\sigma^2$, while in contrast the threshold $s_\infty = \sigma$ is finite because the distribution of the activation energies is bounded.

The relaxation spectrum of a finite-N disordered sample (ring or box of length $L = Na$) can be found numerically by solving the characteristic equation

$$\det(z + \boldsymbol{W}) = 0. \tag{19}$$

The relaxation rate is defined as in Eq. (10). For a given realization of disorder we regard $S_{\circlearrowleft}$ as a free parameter. Making $S_{\circlearrowleft}$ larger means that all the $\mathcal{E}_n$ are increased by the same constant. We define the complexity threshold S_c as the value beyond which the spectrum becomes complex. This means that for $S_{\circlearrowleft} < S_c$ the relaxation is overdamped like in a box, while for $S_{\circlearrowleft} > S_c$ the relaxation is underdamped like in a clean ring. It has been established [16] that

$$S_c = Ns_{1/2}. \tag{20}$$

In the upper panel of Fig. 1 we calculate the dependence of Γ on $S_{\circlearrowleft}$ for a representative disordered ring via direct diagonalization of the $\boldsymbol{W}$ matrix. The results are displayed as blue symbols. The complexity threshold, Eq. (20), is indicated by the left vertical dashed line. In the lower panel of Fig. 1 we calculate the relaxation rate Γ for a box configuration; i.e., one link of the ring has been disconnected. For such a configuration the topological aspect is absent and therefore the spectrum of the N-site sample is real ($S_c = \infty$).

We test whether Eqs. (11) and (12) can be used in order to predict Γ. For this purpose v and D are independently calculated using a standard procedure that is outlined in Appendix A of [17]. Indeed we observe in Fig. 1 a nice agreement between this prediction (solid and dashed green lines) and the previously calculated relaxation rate (blue symbols).

Having realized that Γ of a ring is determined by D via Eq. (11) we would like to understand theoretically the observed nonmonotonic variation as a function of s. In the $N \to \infty$ limit the calculation of D can be carried out analytically [2], using Eq. (A2) of Appendix A. In this limit $D = 0$ in the range $s < s_{1/2}$ where the spectrum is real; then it becomes infinite for $s_{1/2} < s < s_2$, and finite for $s > s_2$. The result of the

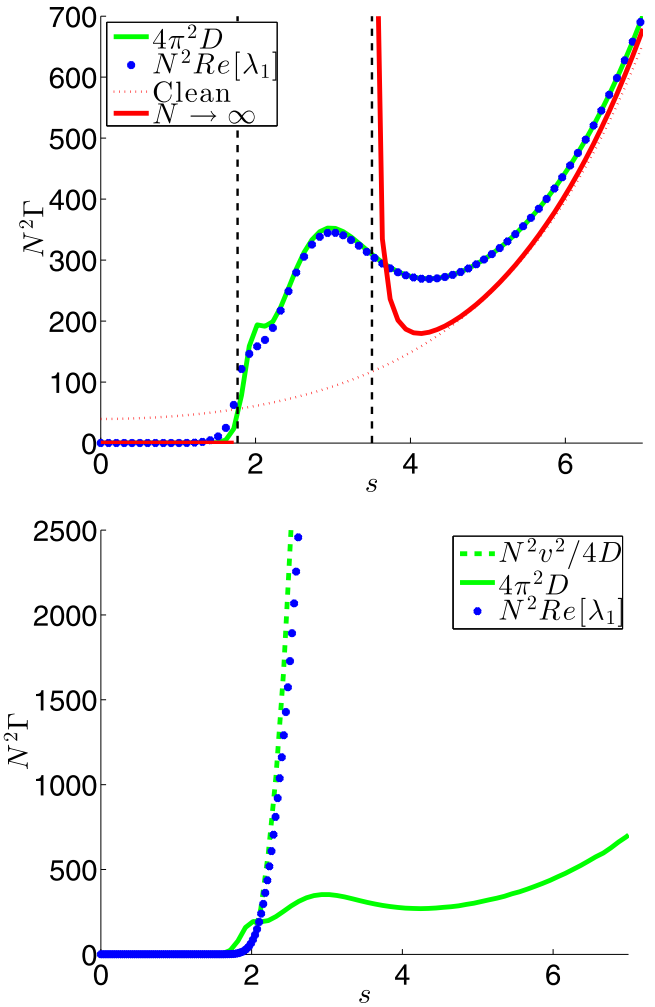

FIG. 1. The relaxation rate $\Gamma = \mathrm{Re}[\lambda_1]$ versus the affinity s for a sample with $N = 1000$ sites, and disorder strength $\sigma = 5$. The units of times are chosen such that $w = 1$. The upper panel is for a ring, while for the lower panel one bond has been disconnected ("box"). The blue data points have been obtained via numerical diagonalization of the $\boldsymbol{W}$ matrix, whereas the solid and dashed green lines are based on Eqs. (11) and (12) with numerically calculated D and v. The red dotted line and the red thick solid line in the upper panel are based on analytical estimates for D, namely, Eqs. (6) and (A2). The vertical dashed lines are the thresholds $s_{1/2}$ (left) and s_2 (right). The former determines S_c via Eq. (20).

calculation in the latter regime is represented by the red curve in the upper panel of Fig. 1. As expected it provides a good estimate only for large s where Eq. (A2) can be approximated by Eq. (A3), leading to

$$\Gamma \approx \left(\frac{2\pi}{N}\right)^2 \frac{w}{2} \exp\left[\frac{1}{2}s - \frac{3}{2}s_{1/2} + s_1\right]. \tag{21}$$

Note that this expression roughly coincides with the clean ring result of Eq. (11) with Eq. (6); see the black curve in the upper panel of Fig. 1.

In the range $s_{1/2} < s < s_2$ the diffusion coefficient is large but finite and becomes N dependent. In [17] a heuristic approach was attempted in order to figure out this N dependence. In the present work we would like to adopt a more rigorous approach. We deduce the N dependence of Γ analytically from the characteristic equation, Eq. (19). We also provide an optional derivation for Eq. (21).

IV. EXTRACTING Γ FROM THE CHARACTERISTIC EQUATION

With the $\boldsymbol{W}$ of the rate equation, Eq. (1), it is possible to associate a symmetric real matrix $\boldsymbol{H}$ as explained in Appendix B. The latter has real eigenvalues $-\epsilon_k$ with $k = 0,1,2,3,\ldots$. Using the identity Eq. (C3) of Appendix C, and setting the units of time such that $w = 1$, the characteristic equation, Eq. (19), is

$$\prod_k (z - \epsilon_k(s)) = (-1)^N 2\left[\cosh\left(\frac{S_{\circlearrowleft}}{2}\right) - 1\right]. \tag{22}$$

Taking the log of both sides, this equation takes the form $\Psi(z) = \Psi(0)$. The identification of the right-hand side as $\Psi(0)$ is based on the observation that $z = \lambda_0 = 0$ has to be an eigenvalue, corresponding to the steady state solution. It is illuminating to regard $\Psi(z)$ as the complex potential in a two-dimensional (2D) electrostatic problem:

$$\Psi(z) = \sum_k \ln(z - \epsilon_k) \equiv V(x,y) + iA(x,y), \tag{23}$$

where $z = x + iy$. The constant $V(x,y)$ curves correspond to potential contours, while the constant $A(x,y)$ curves corresponds to streamlines. The derivative $\Psi'(z)$ corresponds to the field, which can be regarded as either an electric or a magnetic field up to a 90° rotation. On the real axis ($x = \epsilon$, $y = 0$), the potential is

$$V(\epsilon) = \sum_k \ln(|\epsilon - \epsilon_k|) \equiv \int \ln(|\epsilon - \epsilon'|)\varrho(\epsilon')d\epsilon'. \tag{24}$$

The spectral density $\varrho(\epsilon)$ of the eigenvalues $\{\epsilon_k\}$ is further discussed in Appendix D. Using the language of the electrostatic picture we regard it as a charge distribution. For full disorder the density for small ϵ is characterized by an exponent μ, namely, $\varrho(\epsilon) \propto \epsilon^{\mu-1}$. The spectral exponent μ is determined via Eq. (15). An explicit example for the implied dependence of μ on s is provided by inverting Eq. (18). One observes that μ becomes infinite as s approaches $s_\infty = \sigma$. For $s > s_\infty$ a gap is opened. In Appendix E we provide some insight with regard to the implied electrostatic potential $V(\epsilon)$. The bottom line is summarized by Fig. 2. For full disorder, if $s < s_{1/2}$ the envelope at the origin has a positive slope; hence the equation $V(x) = V(0)$ has real solutions, and the relaxation spectrum $\{\lambda_k\}$ comes out real. For $s > s_{1/2}$ the envelope at the origin has a negative slope; hence there are no real solutions at the bottom of the spectrum, and the low eigenvalues become complex. Accordingly the threshold S_c for full disorder is determined by Eq. (20).

We would like to estimate the relaxation rate in the nontrivial regime $S_{\circlearrowleft} > S_c$, where the topology of the ring is reflected. Given the spectral density $\varrho(x)$, the electrostatic potential is

$$V(x,y) = \frac{1}{2}\int \ln[(x - x')^2 + y^2]\varrho(x')\,dx'. \tag{25}$$

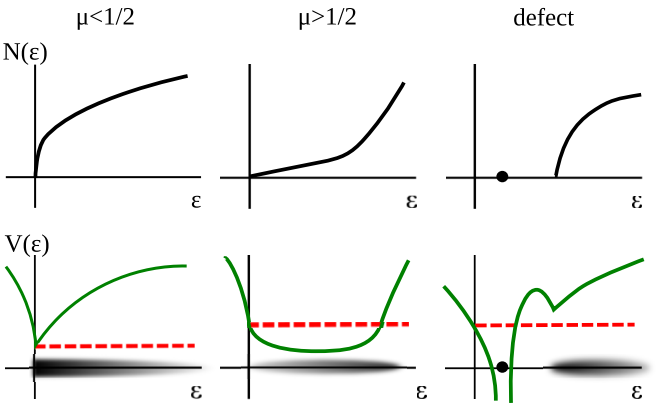

FIG. 2. Caricature of the electrostatic picture used to determine the transition to complexity. The panels of the top row display the integrated density of states that comes from $\varrho(\epsilon)$. The latter is represented by a cloud along the axes of the lower panels. A weak link (defect) contributes an isolated charge at the vicinity of the origin, unlike full disorder (left) that fills the gap with some finite density. The associated envelope of the electrostatic potential is displayed as green lines. The dashed red line is $V(0)$. For $s < s_{1/2}$ the spectral density has exponent $\mu < 1/2$; hence $V'(0)$ is positive, and consequently the equation $V(x) = V(0)$ has real solutions. For $s > s_{1/2}$ the spectral exponent $\mu > 1/2$ implies negative $V'(0)$, and consequently complex roots appear.

Expanding to second order near the origin, we have

$$V(x,y) \approx C_0 - C_1 x + \tfrac{1}{2} C_2 y^2, \tag{26}$$

where the coefficients C_n are defined as

$$C_n = \int_0^\infty \frac{1}{\epsilon^n} \varrho(\epsilon)\, d\epsilon. \tag{27}$$

Notice that $C_0 = V(0)$ and $C_1 = E(0)$ are the potential and the electrostatic field at the origin. To determine the real part of the complex gap it is enough to realize that the equipotential contour $V(x,y) = V(0)$ is approximately a parabola near the origin:

$$x = \frac{1}{2}\frac{C_2}{C_1} y^2. \tag{28}$$

We define as a reference the field line $A(x,y) = 0$ that stretches through the origin along the x axis to $-\infty$. The first excited eigenvalue is determined by the intersection of the $V(x,y) = V(0)$ potential contour with the next field line, namely, with $A(x,y) = 2\pi$. By definition of the stream function $A(x,y)$, which can be regarded as an application of the Cauchy-Riemann theorem, it is equivalent to the requirement of having an enclosed flux

$$\int_0^{\sqrt{2(C_1/C_2)\Gamma}} |\vec{E}(x,y)|\, dy = 2\pi. \tag{29}$$

The integrand is approximated by $|\vec{E}(x,y)| \approx C_1$; hence we deduce

$$\Gamma \approx 2\pi^2 \frac{C_2}{C_1^3}. \tag{30}$$

If all the Cs are proportional to N it follows that $\Gamma \propto N^{-2}$ as in the case of a clean diffusive ring. This is indeed the case if $s > s_2$. But if $s < s_2$ we have to be careful about the lower cutoff. From the quantization condition $\mathcal{N}(\epsilon) = 1$ we deduce that $\epsilon_1 \propto N^{-1/\mu}$ and get

$$\Gamma \propto N^{-\eta}, \qquad \eta = \begin{cases} \frac{1}{\mu}, & \text{for} \quad s_{1/2} < s < s_1, \\ \left(3 - \frac{2}{\mu}\right), & \text{for} \quad s_1 < s < s_2, \\ 2, & \text{for} \quad s > s_2. \end{cases} \tag{31}$$

Comparing with Eq. (11) we realize that consistency requires one to assume that $D \propto N^{(2/\mu)-1}$ for $s_1 < s < s_2$, and $D \propto N^{2-(1/\mu)}$ for $s_{1/2} < s < s_1$. The latter result (but not the former) is in agreement with the heuristic approach of [17]. In the heuristic approach it has been assumed, apparently incorrectly, that the disorder-induced correlation length scales like N throughout the whole regime $s < s_2$ and becomes size independent for $s > s_2$. Apparently the N dependence of the disorder-induced correlation length becomes anomalous within the intermediate range $s_1 < s < s_2$.

The result in Eq. (31) for Γ has an obvious implication on the spectral density of the relaxation modes. Clearly $\mathrm{Re}[\lambda_\nu]$ with $\nu = 0,1,2,3,\ldots$ should be a function of ν/N, reflecting that the spectral density is extensive in N. Accordingly Eq. (31) can be rephrased as saying that $\mathrm{Re}[\lambda_\nu] \propto \nu^\eta$. This result is in general agreement with the heuristic argument of [12], but not in the regime $s_1 < s < s_2$, where it had been argued that $\eta = \mu$ while our result is $\eta = 3 - (2/\mu)$. The maximum difference is for $\mu \sim 1.5$. Our prediction is supported by the numerical example in Fig. 3. We also note that Eq. (28) implies that $\mathrm{Im}[\lambda_\nu] \propto \nu^{\eta/2}$ irrespective of μ. But a numerical inspection (not displayed) shows that the latter approximation works well only for the few first eigenvalues.

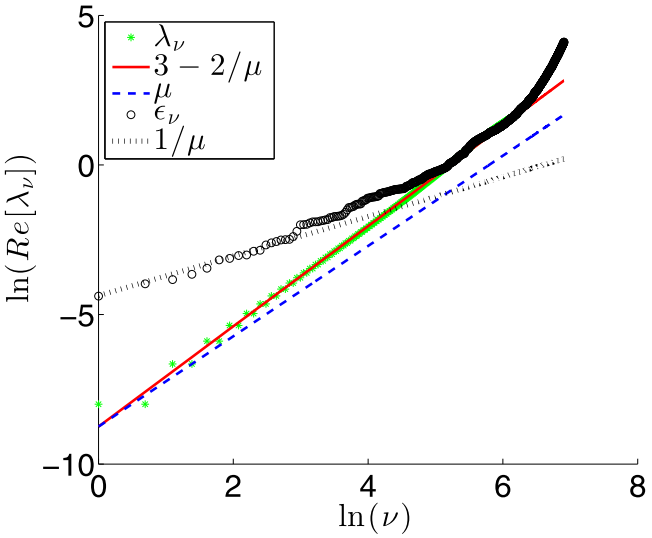

FIG. 3. The ϵ_ν (circles) and the $\mathrm{Re}[\lambda_\nu]$ (stars) versus the index $\nu = 1,2,3,\ldots$ in natural log-log scale for an $N = 1000$-site disordered ring. The strength of the disorder is $\sigma = 5$, and $s = 3.2015$ which implies $\mu = 1.5091$. The expected density $\varrho(\epsilon) \propto \epsilon^{\mu-1}$ at the lower part of the spectrum is confirmed by the agreement with $\epsilon_\nu \propto \nu^{1/\mu}$ (dotted line). We compare the numerical result for $\mathrm{Re}[\lambda_\nu]$ with our prediction $\eta = 3 - (2/\mu)$ (slope of the red solid line) and contrast it with the naive heuristic expectation $\eta = \mu$ (slope of the blue dashed line).

V. SPARSE DISORDER

So far we have considered "full disorder" for which one is able in principle to determine a coarse-grained diffusion coefficient D, that may depend on L, and from that to extract Γ via Eq. (11), leading to Eq. (31). But in practice the disorder might be "sparse," meaning that only a few links are defective. The extreme case is having a single "weak link," meaning a bond or a region where the transitions are extremely slow. In such case Eq. (11) for Γ as well as Eq. (20) for S_c are not physically meaningful. Still we can use the electrostatic picture of the previous sections in order to analyze on equal footing the secular equation. This is demonstrated in the subsequent sections.

To get tangible analytical results we consider a minimal model, namely, a diffusive ring with a single weak-link region. The length of the diffusive region is L, and it is characterized by a diffusion coefficient D_0, while the length of the defective region is L_1, and it is characterized by a diffusion coefficient D_1. We characterize the weak-link region by a "conductance" parameter $g = (D_1/L_1)/(D_0/L)$ and take the limit $L_1 \to 0$, keeping g constant. We find that the threshold S_c does not depend on L as in Eq. (20), but rather reflects g. The characteristic equation implies that $\Gamma \propto 1/L^2$ as for a clean ring, but with a prefactor that depends on g. This dependence is illuminating: it leads to an interpolation between the "ring" result in Eq. (11) and the "box" result in Eq. (12).

VI. RING WITH WEAK LINK

We would like to analyze how the relaxation spectrum is affected once a weak link is introduced into a diffusive ring. We use the continuum limit Eq. (7) for the purpose of deriving the characteristic equation. In a region where $v(x)$ and $D(x)$ are constant, a free-wave solution $\rho(x) \propto e^{i\tilde{k}x-\lambda t}$ has to satisfy the dispersion relation $\lambda = D\tilde{k}^2 + iv\tilde{k}$. It is convenient to use the notation $s = v/D$, which would be consistent with the discrete-lattice convention if the lattice constant were taken as the unit length. Given λ we define k that might be either real or pure imaginary through the following expression:

$$\lambda \equiv \left[k^2 + \left(\frac{s}{2}\right)^2\right]D. \tag{32}$$

The complex wave numbers that correspond to this value are $\tilde{k}_\pm = \pm k - i(s/2)$. In each location the actual stationary solution of Eq. (7) has to be a superposition of clockwise (k_+) and anticlockwise (k_-) waves,

$$\rho(x) = [Ae^{ikx} + Be^{-ikx}]e^{(s/2)x} \tag{33}$$

$$\equiv \psi^+(x) + \psi^-(x). \tag{34}$$

We define the state vector

$$\vec{\psi}(x) \equiv \begin{pmatrix}\rho(x)\\ \partial\rho(x)\end{pmatrix} = \begin{pmatrix}1 & 1\\ i\tilde{k}_+ & i\tilde{k}_-\end{pmatrix}\begin{pmatrix}\psi^+(x)\\ \psi^-(x)\end{pmatrix}. \tag{35}$$

The transfer matrix M that matches the state vector at two different locations is defined via the relation

$$\vec{\psi}(x_2) = M\vec{\psi}(x_1). \tag{36}$$

In a ring with a weak link there are two segments with different diffusion coefficients D_0 and D_1. The continuity of the density $\rho(x)$ and the current $J = -D(x)\partial\rho(x) + v(x)\rho(x)$ implies that the derivative $\partial\rho$ should have a jump such that across the boundary

$$\left.\begin{pmatrix}\rho\\ \partial\rho\end{pmatrix}\right|_1 = \begin{pmatrix}1 & 0\\ 0 & D_0/D_1\end{pmatrix}\left.\begin{pmatrix}\rho\\ \partial\rho\end{pmatrix}\right|_0. \tag{37}$$

We define the matrices

$$U = \begin{pmatrix}1 & 1\\ i\tilde{k}_+ & i\tilde{k}_-\end{pmatrix}, \tag{38}$$

$$T = \begin{pmatrix}e^{i\tilde{k}_+x} & 0\\ 0 & e^{i\tilde{k}_-x}\end{pmatrix}, \tag{39}$$

$$R = \begin{pmatrix}1 & 0\\ 0 & D_0/D_1\end{pmatrix}. \tag{40}$$

For free propagation over a distance L we have $M_0 = UT_0U^{-1}$, with T_0 that involves a wave number k that is determined by D_0. For a weak link we have $M_1 = R^{-1}UT_1U^{-1}R$, where T_1 describes the free propagation in the D_1 region that has some length L_1. It is convenient to define the effective length of the weak link as $\ell = (D_0/D_1)L_1$. The only nontrivial way to take the limit of zero-thickness weak link ($L_1 \to 0$) is to adjust $D_1 \to 0$ such that ℓ is kept constant. This leads to the following result:

$$M_1 = R^{-1}UT_1U^{-1}R = \begin{pmatrix}1 & \ell\\ 0 & 1\end{pmatrix}. \tag{41}$$

The characteristic equation is

$$\det[1 - M_1M_0] = 0, \tag{42}$$

leading to

$$\cos(q) - \frac{1}{2g}\left[q^2 + \left(\frac{S_\circlearrowleft}{2}\right)^2\right]\frac{\sin(q)}{q} = \cosh\left(\frac{S_\circlearrowleft}{2}\right), \tag{43}$$

where we have defined

$$g \equiv \frac{L}{\ell} = \frac{D_1/L_1}{D_0/L} \tag{44}$$

along with $q = kL$ and $S_\circlearrowleft = sL$.

In Fig. 4 we find the dependence of the lowest eigenvalues on $S_\circlearrowleft$ via numerical solution of Eq. (43) and using Eq. (32). The units of length and time are such that $D = L = 1$. From the first eigenvalue we get Γ as defined in Eq. (10). It is implied by the rescaling of the variables in the characteristic equation that $\Gamma \propto 1/L^2$ as for a clean ring. In Fig. 5 we illustrate the dependence of Γ on $S_\circlearrowleft$ and on g. The observed $S_\circlearrowleft$ dependence is monotonic, unlike that of Fig. 1. In the clean-ring limit there is no $S_\circlearrowleft$ dependence because we are considering the continuum limit, setting $D = 1$ irrespective of s, while in Fig. 1 the diffusion coefficient was given by Eq. (6). Irrespective of this presentation issue, as g decreases, the drift-determined s dependence is approached, consistent with Eq. (12). Thus we have a nice interpolation between the "ring" and "box" expressions for Γ.

To determine the threshold S_c for the appearance of complex eigenvalues we take a closer look at Eq. (43). The left-hand

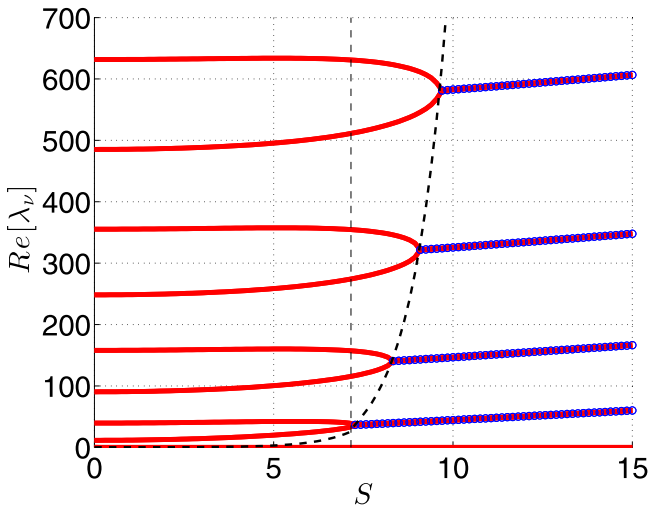

FIG. 4. The lower eigenvalues for a ring with a weak link versus $S \equiv S_{\circlearrowleft}$. The units of length and time are such that $D = L = 1$ and we set $g = 0.2$. For large enough S the eigenvalues become complex and the real parts coalesce (indicated by blue circles). The threshold is indicated by the dashed curve that has been deduced from the envelope of the characteristic equation. The dashed vertical lines indicate S_c of Eq. (46).

side is an oscillating function within an envelope:

$$A(q) = \sqrt{1 + \frac{1}{g^2}\left(\frac{q^2 + (S_{\circlearrowleft}/2)^2}{2q}\right)^2}. \tag{45}$$

This envelope has a minimum at $q = S_{\circlearrowleft}/2$. Accordingly if $A(S_{\circlearrowleft}/2) < \cosh(S_{\circlearrowleft}/2)$ complex eigenvalues appear, and we

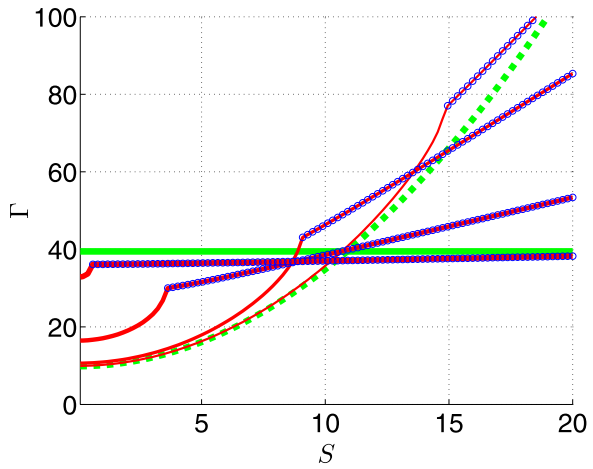

FIG. 5. The relaxation rate Γ for the ring of Fig. 4 versus $S \equiv S_{\circlearrowleft}$. The horizontal solid green line is for a clean ring ($g = \infty$), while the dashed green line is for a disconnected ring ($g = 0$). The other lines are for $g = 10$, 1, 0.1, and 0.01. To the right of each knee the first eigenvalue (λ_1) becomes complex, indicated by the blue circles. This figure should be contrasted with Fig. 1: the significant difference is the nonmonotonic s dependence there (one should not be overwhelmed by the different s dependence in the clean-ring limit; see text).

can deduce the threshold S_c from the equation

$$\sqrt{1 + \left(\frac{S_{\circlearrowleft}}{2g}\right)^2} = \cosh\left(\frac{S_{\circlearrowleft}}{2}\right). \tag{46}$$

To get an explicit expression we solve the approximated equation $S_{\circlearrowleft}/(2g) = \cosh(S_{\circlearrowleft}/2)$ and deduce a solution in terms of the Lambert function,

$$S_c = -2\mathbb{W}(-g/2). \tag{47}$$

This is valid provided $S_{\circlearrowleft} \gg g$, which is self-justified for small g. We can use the same procedure in order to determine the complexity threshold for a given eigenvalue λ in Fig. 4. Recall that the corresponding q is $q^2 = L^2\lambda/D_0 - S_{\circlearrowleft}^2/4$. Solving the quadratic equation $A(q) = \cosh(S_{\circlearrowleft}/2)$ we find the q beyond which the spectrum becomes real again. It terms of λ the explicit expression is

$$\lambda_c = \frac{2D_0}{L^2} g^2 \sinh^2\left(\frac{S_{\circlearrowleft}}{2}\right)\left[1 + \sqrt{1 - \left(\frac{S_{\circlearrowleft}}{2g\sinh\frac{S_{\circlearrowleft}}{2}}\right)^2}\right]. \tag{48}$$

This boundary is indicated by a dashed black line in Fig. 4.

VII. RECONSTRUCTION OF THE CONTINUUM LIMIT

By reverse engineering, requiring consistency between Eq. (43) and Eq. (22), we deduce that the electrostatic potential that is associated with the characteristic equation for a ring with a weak link is

$$V(\epsilon) = \ln\left\{2(\cos(q)-1) - \frac{1}{g}\left[q^2 + \left(\frac{S_{\circlearrowleft}}{2}\right)^2\right]\frac{\sin(q)}{q}\right\}. \tag{49}$$

This potential is plotted in Fig. 6 and labeled as $N = \infty$. We would like to reconstruct this potential by means of Eq. (24). For this purpose we have to find the real eigenvalues of the associated $\boldsymbol{H}$; see Eq. (B6). Formally the equation $\det(z + \boldsymbol{H}) = 0$ is obtained by setting $S_{\circlearrowleft} = 0$ in the right-hand side (RHS) of Eq. (43), leading to

$$\cos(q) - \frac{1}{2g}\left[q^2 + \left(\frac{S_{\circlearrowleft}}{2}\right)^2\right]\frac{\sin(q)}{q} = 1. \tag{50}$$

From Eq. (32) it follows that $\epsilon_k = [q_k^2 + S_{\circlearrowleft}^2/4]D_0/L^2$, where q_k are the roots of the above equation. Using these "charges" we compute $V(\epsilon)$ via Eq. (24) and plot the result in the upper panel of Fig. 6. Some truncation is required, so we repeat the attempted reconstruction with $N = 10$ and $N = 23$ roots. We observe that the result converges to the $N = \infty$ limit. The residual systematic error as ϵ becomes larger is due to finite truncation of the number of roots used in the reconstruction.

The characteristic equation, Eq. (43), parallels the discrete version, Eq. (22). One should be aware that the spectral density contains an "impurity" charge ϵ_0 as illustrated in the third panel of Fig. 2. It is easy to explain the appearance of this exceptional charge using the discrete-lattice language. In the absence of a weak link the diagonal elements of the $\boldsymbol{W}$ matrix are $-\gamma$, where $\gamma = we^{s/2} + we^{-s/2} = 2w\cosh s/2$. The spectrum of the associated $\boldsymbol{H}$ matrix forms a band, such that the lower edge

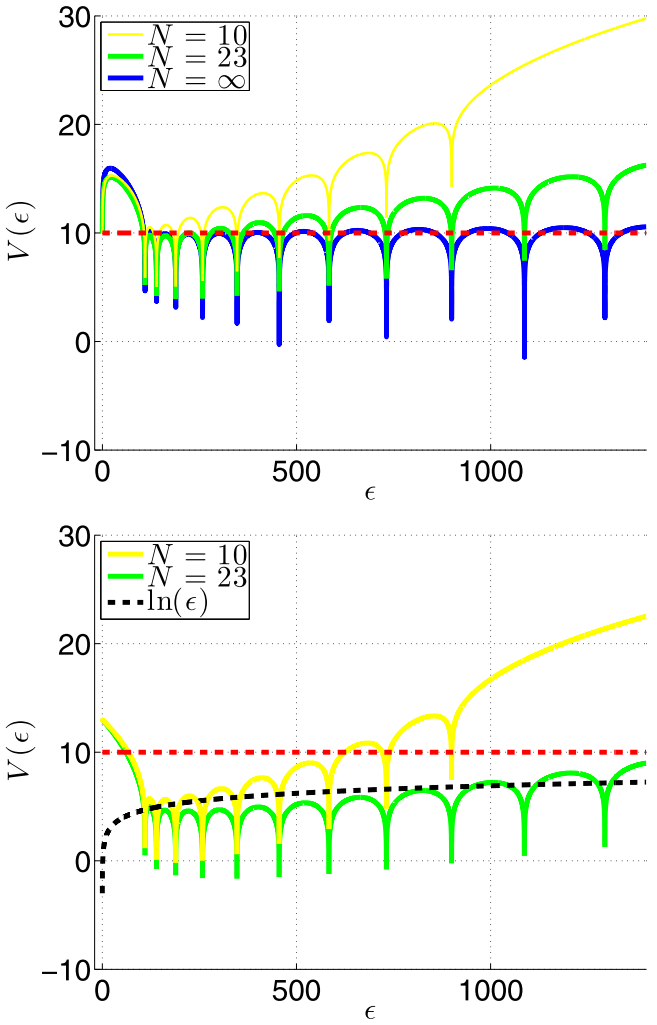

FIG. 6. Electrostatic reconstruction of the characteristic equation of a continuous ring with weak link with $D = L = 1$ and $g = 10^{-3}$ and $S_{\circlearrowleft} = 20$. The blue line is the electrostatic potential of a continuous ring with a defect. The dashed red line is $V(0)$. The yellow and green lines are reconstructions using a finite number of (numerically obtained) charges. By increasing the number of charges that are included in the reconstruction, it is clear that the deviation from the blue line is due to finite size truncation. In the lower panel we display the contribution of the impurity-level charge (dashed black line) and the quasicontinuum charges (the other lines) to the reconstructed potential.

of $\varrho(\epsilon)$ is

$$\epsilon_{\text{floor}} = \gamma - 2w = 2w[\cosh(s/2) - 1]. \tag{51}$$

If we introduce a weak link $w_0 \ll w$ at the (0,1) bond, we get one exceptional diagonal element γ_0. Consequently, for small enough w_0, there is an out-of-band impurity level that does not mix with the band:

$$\epsilon_0 \approx \gamma_0 = w_0 e^{s/2} + w e^{-s/2}. \tag{52}$$

In the lower panel of Fig. 6 we separate the contribution of the impurity level from the contribution of all the other band levels.

VIII. DISCUSSION

We have outlined a physically appealing procedure to extract the relaxation rate of a stochastic spreading process in a closed ring, bridging between the discrete model and its continuum limit, and treating on equal footing full and sparse disorder. By sparse disorder we mean several weak links. For presentation purposes we have provided a full analysis for a ring with a single defect, but the generalization to several weak links is merely a technical issue.

Our approach has been inspired by previous works regarding non-Hermitian Hamiltonians [13–15] and follows our previous publication [16] regarding the determination of the complexity threshold. In the present work the emphasis was on the determination of the relaxation rate Γ in the "complex" regime where the topological aspect manifests itself. Generally speaking in this regime Γ may exhibit anomalous dependence on the length of the sample.

ACKNOWLEDGMENTS

We thank Oleg Krichevsky (BGU) for a helpful discussion. This research has been supported by the Israel Science Foundation (Grant No. 29/11).

APPENDIX A: EXPRESSIONS FOR v AND D IN THE PRESENCE OF DISORDER

In the presence of disorder, the forward and backward rates are random numbers. Here we summarize known analytical expressions for v and D based on [2], using notations as in [16,17]. Taking the infinite chain limit, and using units such that the lattice spacing is $a = 1$, the expression for the drift velocity is

$$v = \frac{1 - \left\langle \frac{\overleftarrow{w}}{\overrightarrow{w}} \right\rangle}{\left\langle \frac{1}{\overrightarrow{w}} \right\rangle}. \tag{A1}$$

We notice that a nonpercolating resistor-network disorder will diminish the drift velocity as expected due to the denominator. Irrespective of that the result above is valid only in the "sliding regime" where $v > 0$. Looking at the numerator one observes that the implied condition for that is $s > s_1$. As for the diffusion, it becomes finite for $s > s_2$, and the explicit expression is

$$D = \frac{1 - \left\langle \frac{\overleftarrow{w}}{\overrightarrow{w}} \right\rangle^2}{1 - \left\langle \left(\frac{\overleftarrow{w}}{\overrightarrow{w}} \right)^2 \right\rangle} \left\langle \frac{1}{\overrightarrow{w}} \right\rangle^{-3} \times \left[\left\langle \frac{1}{\overrightarrow{w}} \right\rangle \left\langle \frac{\overleftarrow{w}}{\overrightarrow{w}^2} \right\rangle + \frac{1}{2} \left\langle \frac{1}{\overrightarrow{w}^2} \right\rangle \left(1 - \left\langle \frac{\overleftarrow{w}}{\overrightarrow{w}} \right\rangle \right) \right]. \tag{A2}$$

For large bias a practical approximation is

$$D \approx \frac{1}{2} \left\langle \frac{1}{\overrightarrow{w}} \right\rangle^{-3} \left\langle \frac{1}{\overrightarrow{w}^2} \right\rangle. \tag{A3}$$

Considering a ring with random rates $we^{\pm \mathcal{E}_n/2}$, the dependence of all the various expectation values on the affinity s is expressible in terms of the parameters w and s_μ. For example,

$$v = e^{\frac{1}{2}(s_1 - s_{1/2})} \left[2 \sinh \left(\frac{s - s_1}{2} \right) \right] w. \tag{A4}$$

APPENDIX B: THE ASSOCIATED *H* MATRIX

Our model is described by a conservative matrix $\boldsymbol{W}$ that describes hopping between sites. In the chain configuration the site index n runs from $-\infty$ to ∞, while in the ring configuration it is defined modulo N. In the latter case we characterize the stochastic field by a potential $U(n)$ and by an affinity $S_{\circlearrowleft}$, such that

$$\mathcal{E}_n = U(n) - U(n-1) + \frac{S_{\circlearrowleft}}{N}. \tag{B1}$$

Then we associate with $\boldsymbol{W}$ a similar matrix $\tilde{\boldsymbol{W}}$ and a real symmetric matrix $\boldsymbol{H}$ as follows:

$$\begin{aligned}
\boldsymbol{W} &= \text{diagonal}\{-\gamma_n(s)\} + \text{off diagonal}\{w_n e^{\pm\frac{\mathcal{E}_n}{2}}\},\\
\tilde{\boldsymbol{W}} &= \text{diagonal}\{-\gamma_n(s)\} + \text{off diagonal}\{w_n e^{\pm\frac{S_{\circlearrowleft}}{2N}}\},\\
\boldsymbol{H} &= \text{diagonal}\{-\gamma_n(s)\} + \text{off diagonal}\{w_n\},
\end{aligned}$$

such that

$$\tilde{\boldsymbol{W}} = e^{\boldsymbol{U}/2}\boldsymbol{W}e^{-\boldsymbol{U}/2}, \tag{B2}$$

where $\boldsymbol{U} = \text{diag}\{U(n)\}$ is a diagonal matrix. The relation between $\boldsymbol{W}$ and $\tilde{\boldsymbol{W}}$ can be regarded as a gauge transformation, and $S_{\circlearrowleft}$ can be regarded as an imaginary Aharonov-Bohm flux. The Hermitian matrix $\boldsymbol{H}$ can be regarded as the Hamiltonian of a particle in a ring in the absence of a magnetic flux. The $\boldsymbol{W}$ of a clean ring[Eq. (3)] and its associated $\boldsymbol{H}$ are

$$\boldsymbol{W} = 2w\left[\cos\left(\boldsymbol{P} + i\frac{s}{2}\right) - \cosh\left(\frac{s}{2}\right)\right], \tag{B3}$$

$$\boldsymbol{H} = 2w\left[\cos(\boldsymbol{P}) - \cosh\left(\frac{s}{2}\right)\right], \tag{B4}$$

while in the continuum limit, Eq. (7) implies that

$$\boldsymbol{W} = -D\boldsymbol{P}^2 + iv\boldsymbol{P}, \tag{B5}$$

$$\boldsymbol{H} = -D\left[\boldsymbol{P}^2 + \left(\frac{v}{2D}\right)^2\right]. \tag{B6}$$

In the absence of disorder the eigenvalues are obtained by the simple substitution $\boldsymbol{P} \mapsto (2\pi/L)\nu$, where ν is an integer.

APPENDIX C: THE CHARACTERISTIC EQUATION

Consider the tridiagonal matrix

$$\boldsymbol{A} = \begin{pmatrix} a_0 & b_1 & 0 & \cdots & c_0 \\ c_1 & a_1 & b_2 & \cdots & 0 \\ 0 & c_2 & a_2 & \cdots & 0 \\ \cdots & \cdots & \cdots & \cdots & \cdots \\ b_0 & 0 & 0 & \cdots & 0 \end{pmatrix} \tag{C1}$$

and associated set of transfer matrices,

$$T_n = \begin{pmatrix} a_n & -b_n c_n \\ 1 & 0 \end{pmatrix}. \tag{C2}$$

Our modified indexing scheme of the elements allows a simpler presentation of the formula for the determinant that appears in [18]:

$$\det[\boldsymbol{A}] = \text{trace}\left[\prod_{n=1}^{N} T_n\right] - (-1)^N\left[\prod_{n=1}^{N} b_n + \prod_{n=1}^{N} c_n\right].$$

From here follows

$$\begin{aligned}
\det(z + \boldsymbol{W}) &= \det(z + \tilde{\boldsymbol{W}})\\
&= \det(z + \boldsymbol{H}) - 2\left[\cosh\left(\frac{S_{\circlearrowleft}}{2}\right) - 1\right](-w)^N.
\end{aligned} \tag{C3}$$

Hence the characteristic equation is Eq. (22).

APPENDIX D: THE SPECTRAL DENSITY $\varrho(\epsilon)$

Consider a ring where the transition rates between neighboring sites are random variables $we^{\pm\mathcal{E}_n/2}$. The equation that describes the relaxation in such a ring in the continuum limit is Eq. (7) with "white disorder." Namely, $v(x)$ has Gaussian statistics with $\langle v(x)v(x')\rangle = \nu_\sigma\delta(x-x')$ where $\nu_\sigma = w^2a^3\text{Var}(\mathcal{E})$. Assuming $D(x) = D_0$, and adding to the disorder an average value v_0, one observes that the diffusion equation is characterized by a single dimensionless parameter. It is customary to define, consistent with Eq. (18),

$$\mu \equiv \frac{2D_0}{\nu_\sigma}v_0 = \frac{2s}{\text{Var}(\mathcal{E})}. \tag{D1}$$

This parameter equals v_0 if we use the common rescaling of units such that $2D_0 = \nu_\sigma = 1$. Then the units of time and of length are

$$[T] = \frac{8D_0^3}{\nu_\sigma^2} = \left[\frac{8}{\text{Var}(\mathcal{E})^2}\right]w^{-1}, \tag{D2}$$

$$[L] = \frac{4D_0^2}{\nu_\sigma} = \left[\frac{4}{\text{Var}(\mathcal{E})}\right]a. \tag{D3}$$

In the absence of disorder, by inspection of Eq. (B6), the spectral density $\varrho(\epsilon)$ is like that of a "free particle" but shifted upwards such that the band floor is $\epsilon_0 = (1/4)v^2/D$. In the presence of Gaussian disorder the gap $[0,\epsilon_0]$ is filled. In scaled units the integrated density of states is [3]

$$\mathcal{N}(\epsilon) = \frac{1}{\pi^2}\frac{L}{J_\mu^2(\sqrt{2\epsilon}) + Y_\mu^2(\sqrt{2\epsilon})}, \tag{D4}$$

where J_μ and Y_μ are Bessel functions of the first and second kind. For any μ the large-ϵ asymptotics gives $\mathcal{N}(\epsilon) \approx (1/\pi)\sqrt{2\epsilon}$ in agreement with the free-particle result. In the other extreme, for small ϵ we get $\mathcal{N}(\epsilon) \propto \epsilon^\mu$. It is also not difficult to verify that the clean-ring spectrum (with its gap) is recovered in the $\sigma \mapsto 0$ limit.

We have verified that for box-distributed $\mathcal{E}_n$ the approximation $\varrho(\epsilon) \propto \epsilon^{\mu-1}$ holds at the vicinity of the band floor. In contrast with a Gaussian distribution μ becomes infinite as s approaches $s_\infty = \sigma$; see Eq. (18). For $s > s_\infty$ a gap is opened.

APPENDIX E: STEP-BY-STEP ELECTROSTATICS

The eigenvalues ϵ_n of $\boldsymbol{H}$ can be regarded as the locations of charges in a 2D electrostatic problem. We would like to

gain some intuition for the associated potential along the real axis. For a point charge at ϵ_1 we have $V(\epsilon) = \ln|\epsilon - \epsilon_1|$. For a uniform charge distribution within $\epsilon \in [a,b]$ we get

$$V(\epsilon) = \frac{1}{b-a}\int_a^b \ln|\epsilon - \epsilon'|\, d\epsilon' = \frac{1}{b-a}[(\epsilon-a)\ln|\epsilon-a| - (\epsilon-b)\ln|\epsilon-b| + (a-b)], \tag{E1}$$

which has a minimum at $\epsilon = (a+b)/2$ and resembles a "soft well" potential. To have a flat floor the density has to be larger at the edges. This is the case for a charge density that corresponds to the spectrum of a clean ring. The locations of the charges are

$$\epsilon_n = 2\left[\cosh\left(\frac{s}{2}\right) - \cos\left(\frac{2\pi}{N}n\right)\right] \equiv \epsilon(k_n) \tag{E2}$$

and the potential along the real axis is

$$V(\epsilon) = \frac{N}{2\pi}\int_0^{2\pi} \ln|\epsilon - \epsilon(k)|dk. \tag{E3}$$

For ϵ within the band, the integrand can be written as $\ln|2[\cos(k_0) - \cos(k)]|$, and accordingly the potential vanishes, reflecting an infinite localization length.

In the continuum limit the charge density in the case of a clean ring behaves as $\varrho(\epsilon) \propto \epsilon^{\mu-1}$ with $\mu = 1/2$ and leads to a flat floor. For general μ one can show [16] that

$$V'(\epsilon) \propto \pi\mu\cot(\pi\mu)\epsilon^{\mu-1} \tag{E4}$$

such that the sign of $V'(\epsilon)$ is positive for $\mu < 1/2$, and negative for $\mu > 1/2$. See Fig. 2 for an illustration. We also illustrate there what happens if we have a clean ring that is perturbed by a defect that contributes a charge in the gap.

For $s > s_\infty$ we have $\mu = \infty$, meaning that a gap is opened. If s is sufficiently large the eigenstates of $\boldsymbol{H}$ are "trivially localized," so the eigenvalues are simply

$$\epsilon_n = \exp[(s + \varsigma_n)/2], \tag{E5}$$

where $\varsigma_n \in [-\sigma,\sigma]$ is uniformly distributed. Accordingly the charge density is $\varrho(\epsilon) = N/\sigma\epsilon$ within an interval $\epsilon \in [a,b]$, where $a = \exp[(s-\sigma)/2]$ and $b = \exp[(s+\sigma)/2]$, leading to

$$V(\epsilon) = \frac{N}{\sigma}\left[\ln(|\epsilon - a|)\ln\left(\frac{\epsilon}{a}\right) - \ln(|\epsilon - b|)\ln\left(\frac{\epsilon}{b}\right) + \mathrm{Li}_2\left(1 - \frac{a}{\epsilon}\right) + \mathrm{Li}_2\left(1 - \frac{b}{\epsilon}\right)\right]. \tag{E6}$$

We would like to calculate the decay rate as described by Eq. (30). To carry out the calculation it is easier to integrate with respect to ς. Expanding Eq. (25) in the vicinity of the origin we get the coefficients

$$C_1 = \frac{N}{2\sigma}\int_{-\sigma}^{\sigma} e^{-(s+\varsigma)/2}d\varsigma = \frac{2N}{\sigma}\sinh\left(\frac{\sigma}{2}\right)e^{-s/2} = Ne^{(s_{1/2}-s)/2}, \tag{E7}$$

$$C_2 = \frac{N}{2\sigma}\int_{-\sigma}^{\sigma} e^{-(s+\varsigma)}d\varsigma = \frac{N}{\sigma}\sinh(\sigma)e^{-s} = Ne^{s_1-s}. \tag{E8}$$

Substitution of C_1 and C_2 into Eq. (30) leads to a result that agrees with Eq. (21).

[1] Y. G. Sinai, Theor. Probab. Appl. **27**, 256 (1983).
[2] B. Derrida, J. Stat. Phys. **31**, 433 (1983).
[3] J. Bouchaud, A. Comtet, A. Georges, and P. L. Doussal, Ann. Phys. **201**, 285 (1990).
[4] J.-P. Bouchaud and A. Georges, Phys. Rep. **195**, 127 (1990).
[5] D. R. Nelson and N. M. Shnerb, Phys. Rev. E **58**, 1383 (1998).
[6] K. A. Dahmen, D. R. Nelson, and N. M. Shnerb, in *Statistical Mechanics of Biocomplexity* (Springer, Berlin, 1999), p. 124.
[7] D. K. Lubensky and D. R. Nelson, Phys. Rev. Lett. **85**, 1572 (2000).
[8] D. K. Lubensky and D. R. Nelson, Phys. Rev. E **65**, 031917 (2002).
[9] M. E. Fisher and A. B. Kolomeisky, Proc. Natl. Acad. Sci. USA **96**, 6597 (1999).
[10] M. Rief, R. S. Rock, A. D. Mehta, M. S. Mooseker, R. E. Cheney, and J. A. Spudich, Proc. Natl. Acad. Sci. USA **97**, 9482 (2000).
[11] Y. Kafri, D. K. Lubensky, and D. R. Nelson, Biophys. J. **86**, 3373 (2004).
[12] Y. Kafri, D. K. Lubensky, and D. R. Nelson, Phys. Rev. E **71**, 041906 (2005).
[13] N. Hatano and D. R. Nelson, Phys. Rev. Lett. **77**, 570 (1996).
[14] N. Hatano and D. R. Nelson, Phys. Rev. B **56**, 8651 (1997).
[15] N. M. Shnerb and D. R. Nelson, Phys. Rev. Lett. **80**, 5172 (1998).
[16] D. Hurowitz and D. Cohen, Sci. Rep. **6**, 22735 (2016).
[17] D. Hurowitz and D. Cohen, Phys. Rev. E **90**, 032129 (2014).
[18] L. G. Molinari, Linear Algebra Appl. **429**, 2221 (2008).